Supermodes of multiple-stripe quantum-well heterostructure laser diodes operated (cw, 300 K) in an external-grating cavity

J. E. Epler, N. Holonyak Jr., R. D. Burnham, T. L. Paoli, and W. Streifer

Citation: Journal of Applied Physics **57**, 1489 (1985); doi: 10.1063/1.334460
View online: http://dx.doi.org/10.1063/1.334460
View Table of Contents: http://scitation.aip.org/content/aip/journal/jap/57/5?ver=pdfcov
Published by the AIP Publishing

Supermodes of multiple-stripe quantum-well heterostructure laser diodes operated (cw, 300 K) in an external-grating cavity

J. E. Epler and N. Holonyak, Jr.
Electrical Engineering Research Laboratory and Materials Research Laboratory, University of Illinois at Urbana-Champaign, Urbana, Illinois 61801

R. D. Burnham, T. L. Paoli, and W. Streifer
Xerox Palo Alto Research Center, Palo Alto, California 94304

(Received 10 August 1984; accepted for publication 10 September 1984)

The far-field supermode patterns of a phase-locked multiple-stripe quantum-well heterostructure (QWH) laser diode are described as a function of injection current and emission wavelength, the latter controlled by an external grating. The external-grating cavity is used to isolate single or multiple supermodes of the multiple-stripe QWH laser ($P_{out} > 170$ mW cw, $\lambda \sim 7400$ Å). The progression of supermode patterns consists of a discrete set of mode configurations for each longitudinal mode of the spectrum. The progression is cyclic with a ~ 2.8-Å period which corresponds to the longitudinal mode spacing of the diode. Under high gain conditions, i.e., near the center of the recombination-radiation spectrum or at higher current levels, continuous tunability is observed with gradual transitions between supermode eigenstates. As the gain is reduced (low current), the number of supermodes observed decreases until only the in-phase pattern, i.e., each emitter at the same phase, remains above threshold. The far-field patterns range from a double-lobe pattern with a 10° peak separation (5 μm between emitter phase reversals) to a narrow ($< 2°$ full angle half power) single-lobe in-phase pattern. The experimental data are compared to the results of coupled-mode analysis.

I. INTRODUCTION

Since the introduction of multiple-stripe quantum-well heterostructure (QWH) lasers[1,2] that operate continuously at room temperature, the power output of these devices[1,3] has begun to rival that of large water-cooled gas lasers. Also, if phase locked, a multiple-stripe laser exhibits a substantially reduced beam divergence[4–6] in the direction parallel to the junction, which increases the maximum attainable intensity. The spectral properties of the output beam can be further enhanced by operating multiple-stripe diodes in an external-grating cavity: Improvements include a narrow linewidth,[7–11] enhanced mode stability,[12,13] broadly tunable (~ 40 meV) wavelength[7] and, of current interest, external control of the transverse and longitudinal modes.[6] In the present paper the transverse modes or "supermodes" of phased-array multiple-stripe lasers are isolated with an external-grating cavity. Beyond previous work,[6] the supermode far-field patterns are presented as a function of injection current level and wavelength, i.e., "position" in the recombination-radiation spectrum.

The behavior of semiconductor laser supermodes has been described earlier using a coupled-mode analysis.[14,15] In this theory the N emitters are regarded as N oscillators coupled by the overlap of the optical field between neighboring emitters. As in the classical case, N distinct mode configurations (supermodes) are possible, each at a slightly different frequency. Experimentally, supermodes have been identified[16] in studies of the spatial dependence of the optical field of a phase-locked array. Using similar laser diodes operated in an external-grating cavity, we have observed phenomena explainable in part by coupled-mode analysis. As the cavity wavelength is scanned through the spectrum (with the grating), a cyclical progression of far-field patterns is observed. Each pattern represents a supermode with a distinct phase and amplitude relationship between emitters. The repetition period of an equivalent set of supermodes (which we call a "supermode progression") is 2.8 Å, which corresponds to the diode longitudinal mode spacing. In the present paper, data are presented illustrating the dependence of the supermode progression upon the relative gain of the multiple-stripe quantum-well active region. The gain is varied either by scanning (with an external grating) the operating wavelength along the recombination-radiation spectrum or by varying the injection current level. In either case the in-phase supermode configuration (all emitters with the same phase) is favored near threshold, while double-lobed higher-order modes predominate in high gain operation.

II. EXPERIMENTAL PROCEDURE

The $Al_{x'}Ga_{1-x'}As$-$Al_xGa_{1-x}As$ ($x' \sim 0.85$, $x \sim 0.22$) QWH crystals of this work are grown by metalorganic chemical vapor deposition (MOCVD) as previously described.[17] The quantum-well size is $L_z \approx 400$ Å as shown by the transmission electron microscope (TEM) image of Fig. 1. In the form of single-stripe lasers this QWH crystal has exhibited excellent short wavelength, high-power performance.[18] Also to be noted, a single-stripe single-well QWH typically exhibits a greater degree of carrier bandfilling[7,19] than conventional double heterostructure lasers, which enhances the wavelength tuning range in external cavity operation. To create the multiple-stripe active region, the p-side confining layer is proton bombarded through a thick photo-

 0021-8979/85/051489-06$02.40

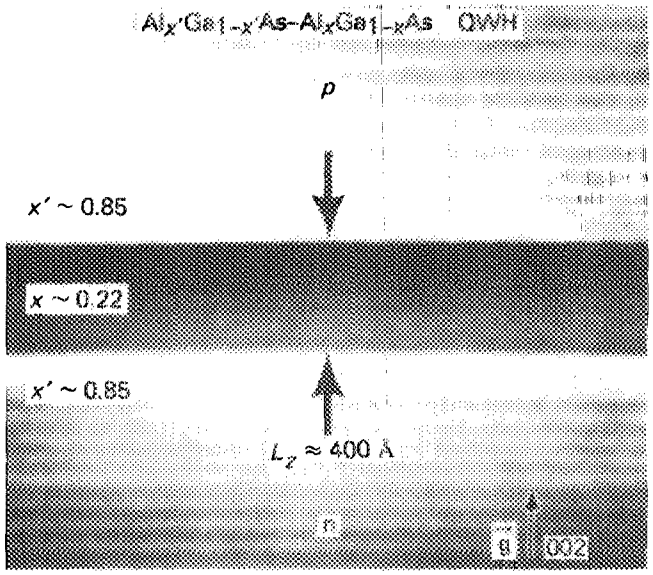

FIG. 1. TEM micrograph of an $Al_{x'}Ga_{1-x'}As$-$Al_xGa_{1-x}As$ quantum-well heterostructure with an $x \simeq 0.22$ quantum well of size $L_z \simeq 400$ Å and confining layers of composition $x' \simeq 0.85$.

resist mask. The crystal is metalized, cleaved into 250-μm bars, and then separated into individual dice. The dice are soldered with In onto small Cu blocks to provide heat sinking and convenient handling. The reflectivity of the diode front facet is modified with an Al_2O_3 antireflecting layer and the back facet with a metalized reflecting coating.

The external cavity shown in Fig. 2 consists of an f 1.0, 50.8-mm focal length lens to collimate the front-facet radiation, and a diffraction grating (7500-Å blaze) to provide dispersed feedback. For single-wavelength operation of multiple-stripe lasers the rulings of the grating are oriented parallel to the junction. In this manner the emission linewidth can be narrowed to within 0.2 Å, sufficient to isolate a single transverse/longitudinal mode. A piezoelectric transducer built into the optical mount permits fine control of the grating angle. The external cavity returns a mirror-inverted image (spectrally dispersed) of the emitter array to the front facet. Thus, the symmetry about the optical axis of the diode near-field pattern is enhanced. For further reference, note that the general behavior of single- and multiple-stripe laser

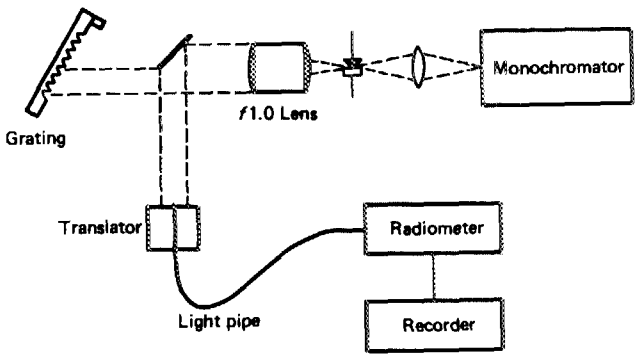

FIG. 2. Diagram of the external-grating cavity and apparatus used to monitor the laser spectrum and far-field patterns of a multiple-stripe QWH laser (Fig. 1). The large aperture lens collimates the front-facet emission and a ruled diffraction grating provides dispersed feedback. The far-field pattern parallel to the crystal layers is recorded with a $\lesssim 0.5°$ resolution.

diodes (excluding supermode phenomena) is given in Ref. 7.

A rectangular Al-coated mirror intercepts a small section of the collimated beam and diverts it onto a small aperture light pipe mounted on a motor-driven translation stage. The optical signal (supermode pattern) is monitored with a radiometer/strip chart recorder (Fig. 2). In this manner, the far-field pattern parallel to the crystal layers can be obtained with a resolution better than 0.5°. The linear scan of the collimated beam introduces an error in the horizontal scale equal to $(\tan x)/x$, which over small angles ($< 30°$, full angle) is negligible. A small fraction of the diode emission escapes the reflective coating and is monitored with a 0.5-m monochromator ($\lesssim 0.2$-Å resolution) equipped with a GaAs-response photomultiplier, and an electrometer/strip-chart recorder. Hence, the emission spectrum and far-field pattern can be simultaneously recorded as indicated in Fig. 2. The back facet of the diode is optically closed off by the reflective coating (a small fraction reaches the monochromator), making it difficult to determine the power output of the overall system. In this case the power output of the front facet is determined by calibrating the integrated intensity of the far-field pattern (with the grating blocked) against the L-I curve of the diode before it is placed in the external cavity. Thus the power outputs quoted below represent the radiation output of the front facet (determined by integrating the far-field scan) and not a true output beam power.

III. EXPERIMENTAL DATA

As the cavity wavelength is scanned between longitudinal modes, the discrete set of far-field patterns shown in Fig. 3 is observed. At this cw current level ($I = 480$ mA $= 1.33 \times I_{th}$) the transition between supermodes is gradual and the tuning is continuous. As the wavelength is increased, we observe that the double-lobed pattern narrows until the peaks merge into a single lobe. After the system (the external grating) is tuned $\Delta\lambda \sim 2.8$ Å, the pattern begins to repeat for the next (adjacent) longitudinal mode. The 2.8-Å period of the progression (i.e., supermode repetition period) corresponds to the 250-μm length of the diode. The first far-field pattern, (a) at 7395.1 Å in Fig. 3, exhibits a 10° separation between lobes in rough agreement with a 5-μm emitter spacing and a 180° phase shift between emitters (the highest-order supermode). As the cavity is tuned toward lower energy, the number of phase shifts (and the mode number) is reduced as predicted by coupled-mode analysis.[14,15] The supermode number ranges from 1 to 20 for a 20-emitter array, and the lobe separation is approximately proportional to the number of phase shifts across the stripes or emitters, which equals $(L\text{-}1)$ where L is the supermode number. For example, the 5.9° lobe separation at 7397.0 Å, (c) of Fig. 3, indicates a ~ 8.3-μm spacing between phase reversals, i.e., a 40% decrease in the number of phase shifts compared with (a). When the cavity is tuned to even longer wavelength, (d) 7397.2 Å, the supermode number approaches 1 (the fundamental, in-phase configuration) and a single-lobe pattern emerges. The full angle half power (FAHP) width of the lobe depends upon the number of modes that coexist, which is shown below to be a function of the optical gain, e.g., current and wavelength. The 5.1° FAHP obviously results from sev-

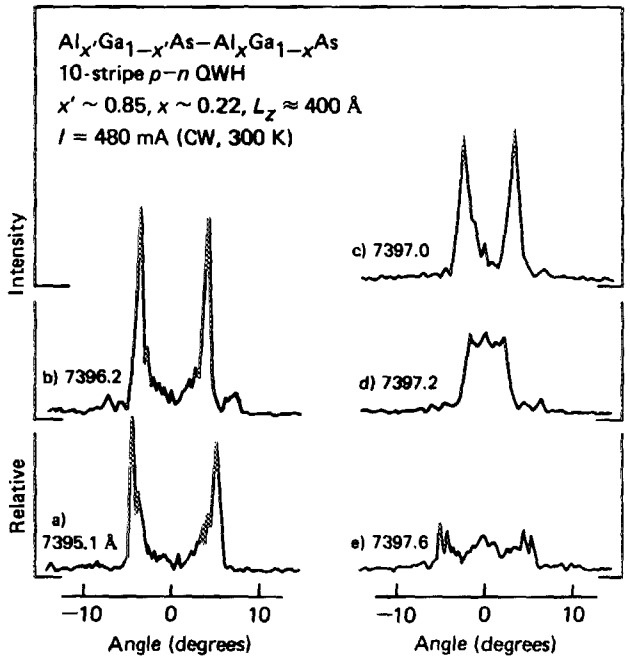

FIG. 3. Progression (series) of far-field supermode patterns, from one longitudinal mode to the next, at the center of the gain profile (7397 Å) for the QWH laser of Fig. 1 at the relatively high cw current level of $1.33 \times I_{th}$ (480 mA). As the cavity wavelength is scanned to slightly longer wavelength with the external grating (Fig. 2), the supermode lobe separation decreases as the number of phase shifts between the multiple emitters is reduced. From (a) to (d), the double peaks have merged into a single lobe although several supermodes coexist. In (e), the out-of-phase supermode coexists with the in-phase supermode. The pattern then begins to repeat with the 2.8-Å period of the longitudinal mode separation. The power output of the diode in (b) is 170 mW.

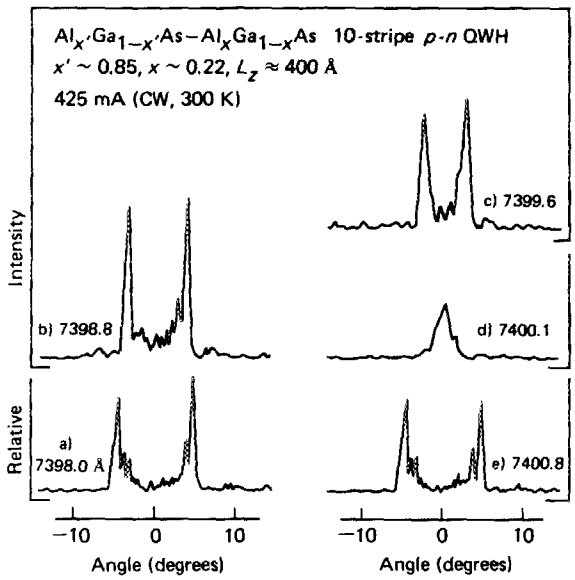

FIG. 4. As the current is reduced from the 480 mA of Fig. 3 to 425 mA ($\lambda \sim 7398$ Å), the number of supermodes decreases; four distinct patterns (a)–(d) are observed. The out-of-phase patterns are similar to the previous figure but the in-phase pattern is better defined with a 2° FAHP. The supermode repetition period is still 2.8 Å.

eral supermodes coexisting. With a further increase in the tuning wavelength, a three-lobed pattern emerges as seen in (e). This is the "seam" between the supermode progressions of adjacent longitudinal modes. For $\lambda > 7397.6$ Å, the progression begins to repeat in the region of the next longitudinal mode. In fact, numerous nearly identical progressions in the supermode patterns are observed as the laser is tuned through this part of the gain profile. Each supermode covers a range of from $\Delta\lambda \sim 0.2$ to ~ 1.0 Å over which it can be tuned. In this manner the discrete set of transverse modes can cover the entire spectral range between longitudinal modes and provide continuous tunability. Note that this has not been previously reported[7] except to a limited extent in Ref. 6. The patterns (a)–(e) all exhibit narrow spectra with linewidths less than 0.4 Å. (Both the resolving power of the external grating and the maximum resolution of the monochromator are approximately 0.2 Å.) When more than one supermode is lasing, as in Fig. 3(d), the linewidth should broaden somewhat because of multiple eigenvalues (multiple propagation constants) of the phased array. However, this has not been observed due mainly to the 0.2-Å resolution limit of the monochromator. Nonetheless, it is apparent that an external grating can be used to control the radiation patterns of a high-power laser [170 mW in Fig. 3(b)] and to isolate the discrete supermodes of the phase-locked laser.

As the current is reduced, the number of supermodes and patterns in the progression decreases; shown in Fig. 4 is the set of supermodes for $I = 425$ mA ($1.18 \times I_{th}$). The four distinct patterns exhibit more sudden transitions between supermodes with a slight gap at 7400.6 Å where no laser operation occurs. The power output is lower and the modes are much "cleaner" than at higher currents, especially the in-phase peak (d). The FAHP of pattern (d) is 2° and the power output is ~17 mW. The general features of the supermode progression of Fig. 4 compared to Fig. 3 is unchanged. As the wavelength is increased, the 10° lobe separation is reduced in discrete steps until an in-phase pattern (d) is formed. Then the progression begins to repeat in the region of the next longitudinal mode. Thus, the similarity of patterns (a) and (e) is not unusual. Generally, even the minute features are reproduced for each longitudinal mode.

The observed supermodes in the same wavelength region but at the lower currents of $I = 380$ and 365 mA are shown in Fig. 5. At the higher of the two currents ($I = 380$ mA) only two supermodes are above threshold. As the wavelength is scanned through the spectrum, the laser emits single-lobed and double-lobed radiation in an alternating cycle. This is typical low gain behavior. A period of the pattern, as before, is 2.8 Å. The separation of the lobes is 5° in pattern (c), which corresponds to phase reversals every 10 μm (the actual stripe spacing of the QWH laser). The power output for the in-phase single-lobe mode (b) is 14 mW and the FAHP is 1.6°.

Just above threshold at $I = 365$ mA, (a) of Fig. 5, only the in-phase supermode is observed. The power output (stimulated emission) is 13 mW and the FAHP is 1.4°. The Fourier transform of an in-phase array of 100-μm width predicts a much narrower beam (0.5). However, the resolution of the monitor is $\lesssim 0.5°$, and the diode operation is near threshold, so that the spatial extent of the stimulated optical field is less than 100 μm. The in-phase pattern shown in Fig. 5 is quite stable and can be tuned over a 10-meV range centered at 7410 Å, with a narrow 0.2-Å linewidth. Again, the

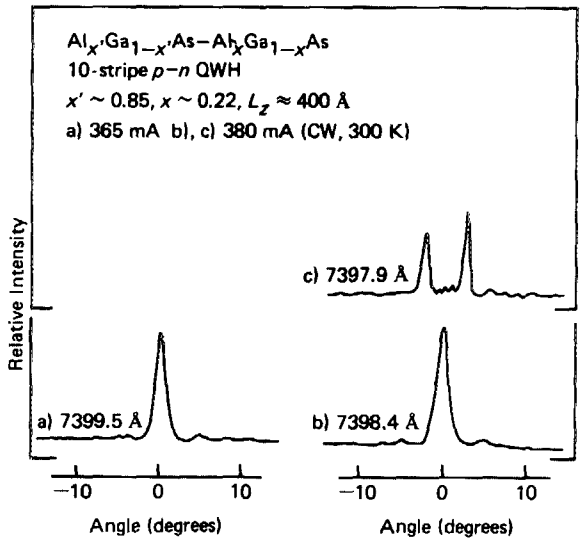

FIG. 5. At the low cw current of 380 mA, only two supermode patterns are observed, a narrow in-phase pattern (1.5° FAHP) and an out-of-phase pattern corresponding to phase reversals spaced at 10 μm apart. As the current is lowered further to just above threshold, only the in-phase pattern is observed and large (2 Å) gaps exist in the spectrum where no lasing occurs. The supermode repetition period remains ~2.8 Å. The power output of the diode in (a) is ~13 mW.

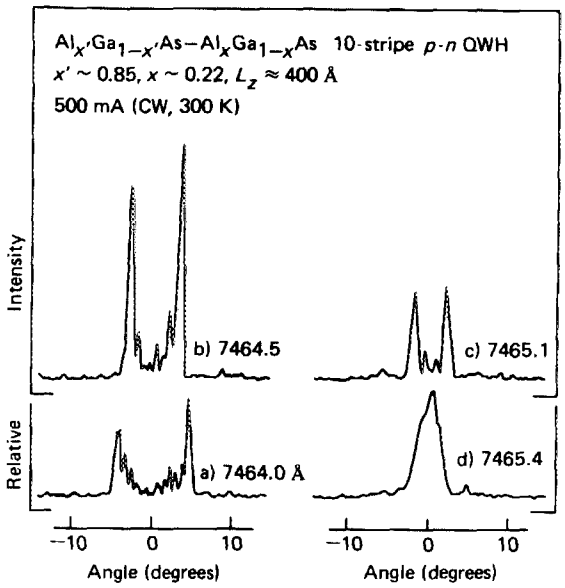

FIG. 7. Supermode far-field patterns at the same current (I = 500 mA) as in Fig. 6 but in a shorter wavelength region (λ = 7465 Å) where the gain is significantly greater. Instead of two, four distinct supermodes are observed as in Fig. 4. The power output of the diode for the in-phase pattern is 55 mW.

repetitive tuning pattern is observed: lasing is observed over a $\Delta\lambda \sim 1$ Å range and then no lasing for the remainder of the 2.8-Å period.

The dependence of the supermode configurations upon the optical gain is observed also as the diode is tuned with the grating through the gain profile, i.e., to higher and higher gain, with the current held constant. In Fig. 6 the diode is operated at a high current (500 mA) and is tuned to the long wavelength edge of the gain profile. At (a) it is just above threshold. For wavelengths longer than 7482 Å, only the in-phase supermode is observed (low gain). As the laser diode is tuned to shorter wavelength with the grating, the gain steadily increases and additional supermodes appear. Thus the longitudinal mode at 7479 Å exhibits a two-pattern progression: an out-of-phase pattern (c) with a 5° lobe separation is observed and an in-phase pattern (b) with a 14-mW output and a FAHP of 2°. Comparison with Fig. 5 (the intensity scale is the same) suggests that the gain is the dominant factor affecting the supermode progression. Note that the wavelength of laser operation is important only because the gain is wavelength dependent.

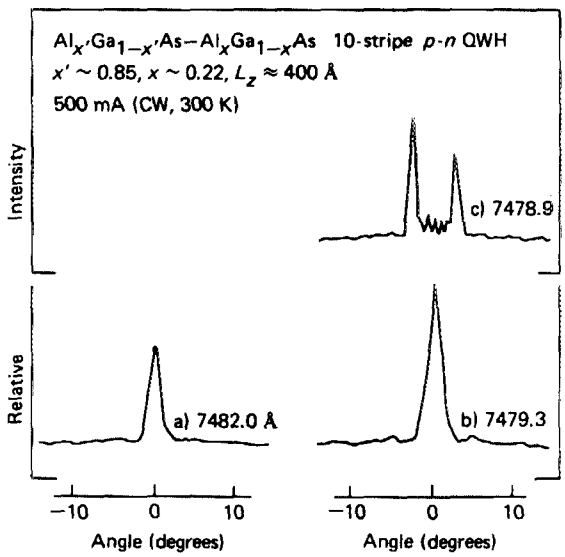

FIG. 6. At the high cw current of I = 500 mA but with the operation grating tuned near the edge of the gain profile (λ = 7482 Å), only the in-phase pattern is observed for $\lambda > 7480$ Å. This illustrates the dependence of the patterns upon the optical gain in the active region. At the slightly shorter wavelength of λ = 7479 Å, the gain is slightly greater, and a second supermode reaches threshold [similar to (b) and (c) in Fig. 5]. The power output of the diode is ~12 mW.

As the cavity wavelength approaches the gain maximum at 7410 Å more supermodes appear. In Fig. 7, four mode configurations are shown, and again the tuning is nearly continuous (from longitudinal mode to longitudinal mode) with only small gaps in the spectrum. As the cavity is tuned toward still shorter wavelength and higher gain, the number of mode configurations approaches six (similar to Fig. 3 of Ref. 6). Then as the wavelength is tuned with the grating through the gain maximum, the supermodes begin to disappear (in number) as the gain decreases. Only the in-phase pattern is observed at the short wavelength edge of the gain profile where the laser is just above threshold.

IV. DISCUSSION

The influence of optical gain, which depends on the excitation level and recombination-radiation spectrum (wavelength), upon the form and number of supermodes is clear (Figs. 3–7). At present, however, the analytical model of supermodes is not sufficient to account fully for their behavior. Nevertheless, visual observations[20] of laser diode near-field configurations in conjunction with the above far-field data reveal the basic character of the phased array. Just above laser threshold the stripe emitters near the center of the array tend to coalesce into a band (~30 μm wide) which

results in a single-lobe pattern. This behavior apparently gives a minimum threshold condition and explains the breadth of the in-phase pattern (1.5° FAHP). As the wavelength is scanned via the external-grating cavity, the active region separates into individual emitters *if the gain is sufficient*. The next lowest threshold mode (still relatively low excitation level but above threshold) operates on an alternating phase with ~ 10-μm centers, which is plausible in view of the built-in 10-μm stripe spacing. At higher gains the "oscillator" strengths are greater (P_{out} is increased by a factor of 10 or more above the conditions near threshold), and the emitters are distinct at a spacing of $\sim 5\,\mu$m, at least for that part of the spectrum in which the lobe separation is $> 5°$. For example, the 5° lobe separations of Figs. 5 and 6 at lower currents are based properly on the 10-μm stripe spacing built into the laser diodes, but as the gain is increased (Figs. 4 and 7, i.e., higher excitation), the periodicity of the active region is changed into a "harmonic" or a 5-μm spacing between emitters. The proton bombardment delineation of the diode structure raises the resistivity of the GaAs cap layer between the stripes and creates an array of current channels into the active region; however, extensive current spreading[21] in the lateral direction between the stripes, especially in a gain-guided structure, serves to smear the injected carrier profile. Because of the smearing, the optical gain between the stripes is somewhat less than at the stripe center but is sufficient to support an emitter if the diode is operating significantly above threshold. Thus at sufficiently high current the far-field patterns can exhibit a 10° lobe separation in accordance with an emitter spacing of $\sim 5\,\mu$m. (Actually Fourier analysis predicts a 10° lobe separation at 7400 Å for a 4.25-μm emitter spacing.) Apparently, the nature of the active region is similar in some regards to a broad area laser with a slab dielectric waveguide: an increase in frequency away from the longitudinal mode frequency induces a higher-order transverse mode (more emitters) in order to satisfy the wave equation. Also, the width of the emitter array can impose boundary conditions that are satisfied only by the observed set of modes. For each value of optical gain (current or wavelength) only a few of the possible 20 supermodes can lase, e.g., roughly five in Fig. 3 and only one in Fig. 5(a).

Clearly, the grating cavity plays a role in adding external coupling to the stripes. The feedback tends to symmetrize the optical field about the optical axis. In addition, the focusing properties of different supermodes varies. The in-phase supermode would be slightly favored because of a smaller "spot size." This effect may partially explain the observation that the in-phase pattern has the lowest threshold. The external cavity should not affect the fundamental internal mechanics of the phased array, except for reduced carrier lifetime where the stimulated emission (photon density) is greatest, but serves to isolate and stabilize the supermode configurations. Further study of both near and far fields of various types of phased-array laser diodes is necessary to develop a comprehensive picture of this phenomenon.

V. CONCLUSIONS

The coupling of an external-grating cavity to a quantum-well laser diode has produced several significant results. First, the combination of broad tunability, high-power output, and narrow linewidth is promising for practical laser sources. Second, the use of multiple-stripe diodes improves the power output and beam divergence of such a system although at some loss in tunability. Finally, the external cavity allows one to isolate the discrete mode configurations of a phased array, thereby providing external control of the radiation pattern and permitting detailed study of supermode phenomena. Using the external-grating cavity, we are able to determine the qualitative dependence of the supermode progression upon the optical gain. For currents less than $1.2 \times I_{th}$, we obtain in-phase patterns with narrow beam divergences ($< 2°$, parallel to the crystal layers). The power output (cavity flux) is approximately 70 mW in the narrow in-phase mode (supermode). At higher currents, and thus greater optical gain, the in-phase supermode cannot be isolated and the beam divergence increases. However, the out-of-phase modes remain well formed with high cw power outputs of over 170 mW.

ACKNOWLEDGMENTS

For technical assistance the authors wish to thank Y. K. Moroz, B. L. Marshall, R. T. Gladin, and B. L. Payne (Illinois), and H. Chung, R. D. Yingling, Jr., F. Endicott, R. L. Thornton, M. Bernstein, W. Mosby, J. Tramontana, J. Walker, G. L. Harnagel, R. Ridder, and A. Alimoda (Xerox). They are grateful to J. M. Brown for Fig. 1 (from Ref. 7). The work of the Illinois group has been supported by NSF Grant No. ECS 82-00517, Army Research Office Contract No. DAAG-29-82-K-0059, and NSF Grant No. DMR 80-20250.

[1]D. R. Scifres, R. D. Burnham, and W. Streifer, Appl. Phys. Lett. **41**, 118 (1982).
[2]N. Holonyak, Jr., R. M. Kolbas, R. D. Dupuis, and P. D. Dapkus, IEEE J. Quantum Electron. **QE-16**, 170 (1980).
[3]D. R. Scifres, C. Lindström, R. D. Burnham, W. Streifer, and T. L. Paoli, Electron. Lett. **19**, 169 (1983).
[4]D. R. Scifres, R. A. Sprague, W. Streifer, and R. D. Burnham, Appl. Phys. Lett. **41**, 1121 (1982).
[5]D. R. Scifres, W. Streifer, R. D. Burnham, T. L. Paoli, and C. Lindström, Appl. Phys. Lett. **42**, 495 (1983).
[6]J. E. Epler, N. Holonyak, Jr., R. D. Burnham, T. L. Paoli, and W. Streifer, Appl. Phys. Lett. **45**, 406 (1984).
[7]J. E. Epler, N. Holonyak, Jr., J. M. Brown, R. D. Burnham, W. Streifer, and T. L. Paoli, J. Appl. Phys. **55**, 670 (1984).
[8]J. A. Rossi, S. R. Chinn, and H. Heckscher, Appl. Phys. Lett. **23**, 25 (1973).
[9]H. Bachert. A. P. Bogatov, P. G. Eliseev, A. Keiper, and K.-A. Khairetdinov, IEEE J. Quantum Electron. **QE-15**, 786 (1979).
[10]R. Wyatt and W. J. Devlin, Electron. Lett. **19**, 110 (1983).
[11]E. Patzak, A. Sugimura, S. Saito, T. Mukai, and H. Olesen, Electron. Lett. **19**, 1026 (1983).
[12]T. L. Paoli, J. E. Ripper, A. C. Morosini, and N. B. Patel, IEEE J. Quantum Electron. **QE-11**, 525 (1975).
[13]M. W. Fleming and A. Mooradian, IEEE J. Quantum Electron. **QE-17**, 44 (1984).
[14]J. K. Butler, D. E. Ackley, and D. Botez, Appl. Phys. Lett. **44**, 293 (1984).
[15]E. Kapon, J. Katz, and A. Yariv, Opt. Lett. **10**, 125 (1984).
[16]T. L. Paoli, W. Streifer, and R. D. Burnham, Appl. Phys. Lett. **45**, 217 (1984).
[17]R. D. Burnham, D. R. Scifres, and W. Streifer, Appl. Phys. Lett. **41**, 228 (1982). See also R. D. Dupuis, L. A. Moudy, and P. D. Dapkus, in *Proceedings of the 7th International Symposium on GaAs and Related Compounds, St. Louis, 1978*, edited by C. M. Wolfe (Institute of Physics, Lon-

don, 1979), pp. 1–9.
[18]R. D. Burnham, C. Lindström, T. L. Paoli, D. R. Scifres, W. Streifer, and N. Holonyak, Jr., Appl. Phys. Lett. **42**, 937 (1983).
[19]J. E. Epler, N. Holonyak, Jr., R. D. Burnham, C. Lindström, W. Streifer, and T. L. Paoli, Appl. Phys. Lett. **43**, 740 (1983).
[20]J. E. Epler, N. Holonyak, Jr., R. W. Kaliski, R. D. Burnham, T. L. Paoli, and W. Streifer (unpublished).
[21]W. T. Tsang, J. Appl. Phys. **49**, 1031 (1971).